Leptons-Enriched Signatures for Semi-Visible Jets

Cesare Cazzaniga

ETH Zürich, Institute for Particle Physics and Astrophysics, CH-8093 Zürich, Switzerland

Abstract

The Hidden Valley scenario proposes alternative BSM models leading to new loosely constrained collider signatures, and possibly explain the nature of Dark Matter and solving the hierarchy problem. Under the assumption of a QCD-like confining dark sector, novel experimental signatures emerge, characterized by sprays of particles resembling hadronic jets containing stable invisible dark matter bound states. These semi-visible jets have been studied theoretically and experimentally in the fully hadronic signature where the unstable composite dark matter can only decay promptly back to Standard Model quarks. We present two simplified models allowing the decays of the unstable dark bound states to electrons and muons, as well as enhanced decays to tau leptons. The resulting signature is characterised by non-isolated leptons inside semi-visible jets. We show the constraints on our models from existing CMS and ATLAS searches, and propose possible realistic analysis strategies leveraging the enhanced leptonic content of these anomalous jets.

1. INTRODUCTION

The presence of dark matter in the universe (DM) [1, 2] represents one of the most outstanding evidence for physics beyond the Standard Model (SM). Nonetheless, the nature of DM itself is not known, and the most common scenarios invoking Weakly Interacting Massive Particles (WIMPs) [3, 4] as DM candidates have been constrained experimentally in large part of their parameter space. In the specific case of the Large Hadron Collider (LHC), WIMPs searches looking for significant missing transverse momentum ($\not{E}_T$) recoiling against visible objects, such as jets [5, 6], photons [7], leptons [8, 9, 10], top quarks [11, 12] or a Higgs boson [13, 14] ($\not{E}_T$+X signatures) have not found any significant excess with respect to SM prediction.

The Hidden Valley scenarios (HV) [15] propose alternative, well-motivated BSM models compatible with the explanation of the DM nature [16, 17, 18], and the solution of the little hierarchy problem [19]. Namely, in the HV scenario, the SM is accompanied by a Hidden sector and connected with it via a heavy and/or weakly coupling mediator. If realised in nature, the HV scenario may result in unusual and little-studied phenomena at the LHC beyond the conventional $\not{E}_T$+X signatures. In the case of a confining Hidden sector charged under $SU(N_c)_{dark}$, jetty final states can be recovered at small 't Hooft couplings $N_c g_{dark}^2 \ll 1$ [20, 21], where g_{dark} is the Hidden sector coupling. This QCD-like regime is the best understood from a theoretical perspective, and current Monte Carlo event generators can reliably simulate HV models within this scenario [20, 21]; there is also a growing effort towards simulating HV models at intermediate [22, 23] and large [24, 25] 't Hooft couplings. Within the QCD-like regime, novel experimental signatures emerge, characterized by sprays of particles resembling hadronic jets that include dark bound states and their decay products to SM quarks (dark jets). Dark jets can appear in the detector at different distances according to the lifetime of the hidden sector bound states. In long-lived dark bound states, displaced signatures arise, such as emerging jets [26] and trackless/displaced jets [27]. For prompt decays of the dark sector bound states to SM particles, typical signatures are prompt dark jets [28, 29] or semi-visible jets (SVJ) [30, 31, 17]. In particular, semi-visible jets occur if a sizable fraction of the dark bound states within the dark jets remains stable, resulting in a multijet+$\not{E}_T$ signature characterized by $\not{E}_T$ aligned with one of the jets.

Fully hadronic semi-visible jets have been searched from the CMS and ATLAS collaborations in the resonant [32] and non-resonant [33] production modes, respectively. No significant excess from the SM prediction has been found. In [34, 35], we propose two simplified models leading to two new SVJ-like signatures enriched in non-isolated leptons. We show that the current LHC searches have no sensitivity to such models, and we propose possible analysis strategies able to probe such unexplored phase space.

2. NEW COLLIDERS SIGNATURES AND SIMPLIFIED MODELS

Semi-visible jets have been studied theoretically and experimentally in the fully hadronic signature where the unstable composite dark bound states can only decay promptly back to Standard Model quarks [30]. The model to produce such signature (fully-hadronic SVJs) assumes a leptophobic Z' portal connecting the SM and the HV sectors. We propose two new simplified models allowing the dark bound states prompt decays into oppositely charged leptons, resulting in SV jets enriched in non-isolated leptons. The first model [34] (SVJℓ) predicts the decay of dark vector mesons in all lepton flavours using two distinct portals for the
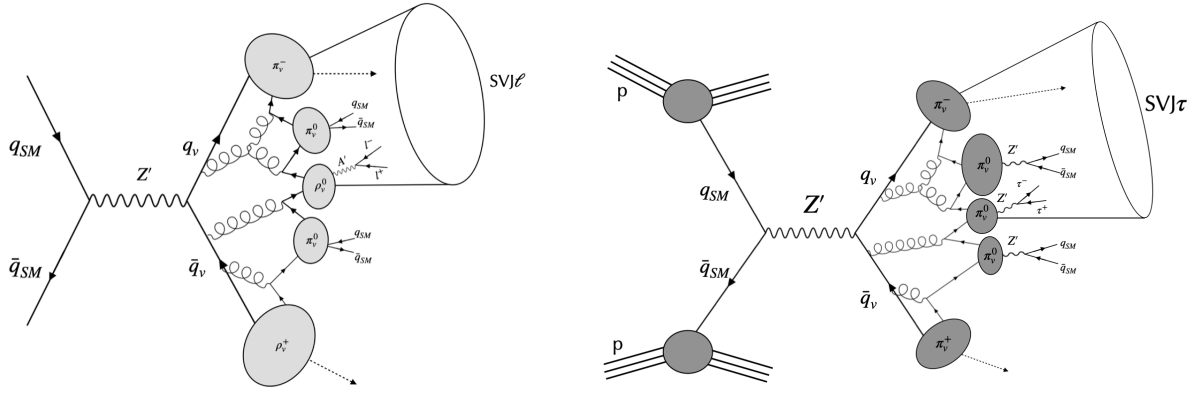
FIGURE 1: *Left panel*: s-channel production of semi-visible jets with non-isolated prompt leptons of all flavours produced from dark hadrons decays (SVJℓ signature, Figure from [34]). *Right panel*: s-channel production of semi-visible jets with τ leptons from dark hadrons decays (SVJτ signature, Figure from [35]).

production of dark quarks and the decays of the dark bound states. On the other hand, the second model [35] (SVJτ) is based on a single portal enhancing the decays of dark pseudo-scalar mesons to τ leptons.

For both models proposed, the confining Hidden sector is charged under $SU(3)_{\text{dark}}$ with two dark quarks flavours, and has three main parameters impacting the collider phenomenology: Λ_{v} (dark sector confinement scale), r_{inv} (fraction of invisible dark bound states), $m_{\text{dark}}/\Lambda_{\text{v}}$ (lightest dark hadron to dark sector confinement scale ratio). Further parameters related to the portals are then introduced according to the models.

2.1. SVJℓ Model and Signature

In this simplified model, two mediators are connecting the SM with the hidden sector: a TeV scale leptophobic Z' coupling both to SM quarks and dark quarks q_{v}, and a lighter dark photon A' coupling both to dark quarks and SM fermions (quarks and leptons). The messenger sector Lagrangian allowing the coupling to SM leptons is:

$$\mathcal{L}_{A'} = -\frac{1}{4} F_{\mu\nu}[A'] F^{\mu\nu}[A'] + \frac{1}{2} M_{A'}^2 A'_\mu A'^\mu - \epsilon e Q A'_\mu J^\mu_{q,\text{SM}} - \epsilon e Q A'_\mu J^\mu_{l,\text{SM}} - g^v_{A'} A'_\mu J^\mu_{\text{v}}, \tag{1}$$

where J^μ_{v} is the dark quarks vector current, $J^\mu_{q,\text{SM}}$ is the SM quarks vector current and $J^\mu_{l,\text{SM}}$ is the SM leptons vector current. Due to the mass hierarchy between A' and Z', the dark vector mesons ρ_{v} will decay predominantly via the A' to SM leptons and quarks. The kinetic mixing portal parameter ϵ in equation (1) governs the coupling strength of the A' to the SM. Due to the nature of the A' portal, the vector mesons are expected to decay democratically to all lepton flavours. The immediate consequence of this two messenger fields model is a factorization between the production of the dark quarks, which a heavy leptophobic Z' boson can mediate, and the decays of the dark vector mesons, which are driven by the lighter A'. In Figure 1, it is sketched the production mechanism of semi-visible jets with inside pairs of opposite charge leptons produced by the unstable dark hadrons. The constraints on the mixing parameter ϵ from the current dilepton resonance searches, displayed in Figure 2, suggest that prompt decays of the dark vector mesons are still possible from few GeV bound state masses and above.

2.2. SVJτ Model and Signature

Differently from the previous model, in this case a unique portal Z' connects the SM and the hidden sector. The general interactions of the Z' boson are contained in the following Lagrangian density:

$$\mathcal{L}_{Z'} = -Z'_\mu \bar{u}_i \gamma^\mu \left(g^{u_R}_{ij} P_R + g^{u_L}_{ij} P_L \right) u_j - Z'_\mu \bar{d}_i \gamma^\mu \left(g^{d_R}_{ij} P_R + g^{d_L}_{ij} P_L \right) d_j$$
$$- Z'_\mu \bar{e}_i \gamma^\mu \left(g^{e_R}_{ij} P_R + g^{e_L}_{ij} P_L \right) e_j - Z'_\mu \bar{q}_{\text{vi}} \gamma^\mu \left(g^{q_{\text{v}R}}_{ij} P_R + g^{q_{\text{v}L}}_{ij} P_L \right) q_{\text{vj}}. \tag{2}$$

The following benchmark for the coupling matrices is chosen:

$$g^{d_R}_{ij} = g^{d_L}_{ij} = g^{u_L}_{ij} = g^{e_L}_{ij} = 0, \quad g^{u_R}_{ij} = g_u \delta_{ij},$$
$$g^{e_R}_{ij} = g_\tau \delta_{i3}\delta_{j3}, \quad g^{q_{\text{v}R}}_{ij} = g^{q_{\text{v}L}}_{ij} = g_{q_{\text{v}}} \delta_{ij}. \tag{3}$$

Within such benchmark, below the $b\bar{b}$ threshold, the unstable dark pseudo-scalar mesons decay predominantly to c quarks and τ leptons. The relative contributions between these two decay modes depend on the relative strength of the couplings g_u and g_τ. In

order to probe the impact of having unstable dark bound states decaying to τ leptons we have introduced an effective parameter BR_τ depending on the ratio g_u/g_τ. Such parameter controls also the invisible component of the final states, since a larger amount of neutrinos is expected when the fraction of dark bound states decay to τ leptons, gets larger. The proposed simplified model allows for s-channel production of semi-visible jets with an enriched τ lepton content, originating from the unstable dark pseudo-scalar mesons, as illustrated in Figure 1. The constraints from the current LHC searches on the SVJτ model are displayed in Figure 2; at low mass the major constraints come from ditau searches, while at high mass the CMS SVJ search imposes the tighter limit on g_u.
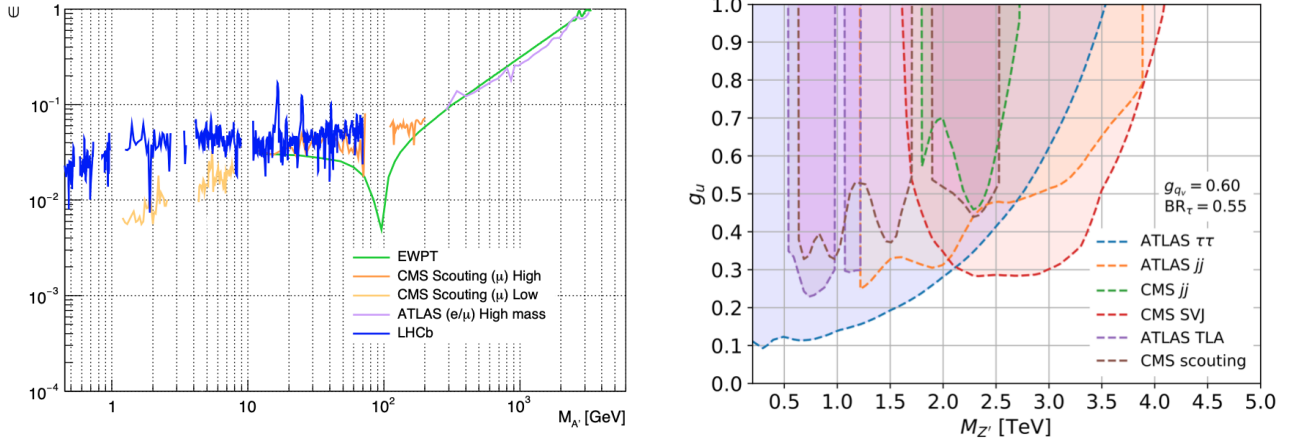

FIGURE 2: Constraints from the current LHC searches on the SVJℓ and SVJτ models. *Left panel*: constraints on the kinetic mixing parameter ϵ for A' in the SVJℓ model from the Electroweak Precision Test [36] (EWPT) and five searches including the high-mass ATLAS dilepton search [37], the intermediate-mass CMS dilepton search [38], the low-mass data-scouting CMS search [39] and the LHCb dark photon search [40]. *Right panel*: constraints on the coupling of Z' to quarks g_u for the SVJτ model from six searches including the dijet search by ATLAS [41], the dijet search by CMS [42], the ditau search by ATLAS [43], the SVJ search by CMS [44], the trigger-object-level analysis (TLA) search by ATLAS [45] and the dijet data-scouting search by CMS [46].

3. EXPERIMENTAL HANDLES AND STRATEGIES

The enriched leptonic content of the signal jets for the SVJℓ and SVJτ signatures implies both reassessing the efficiency of the fully-hadronic resonant SVJ search from CMS [32], and developing new techniques to exploit the anomalous leptonic content of signal jets fully. In the following, we will summarise the current SVJ analysis strategy's main limitations and propose ways to improve it to tackle the proposed signatures using new specialized observables and considering alternative trigger strategies.

3.1. Current Limitations of the Fully-Hadronic Resonant SVJ Search

Both the proposed simplified models, as shown in Figure 1, imply looking for a broad high mass resonance appearing over a falling background in the dijet transverse mass spectrum m_T [32]. Therefore, the CMS inclusive search must be taken as a standard candle to assess if the new signatures are covered from such analysis. We have found that two specific requirements from the CMS analysis relying on the signal features are expected to wash out its sensitivity for the proposed new signatures.

The first limitation comes from a veto requirement on mini-isolated leptons in the event. Compared to standard isolation, which quantifies the hadronic activity around a given lepton in a cone of fixed size, mini-isolated assesses such activity by adapting the cone size according to the transverse momentum p_T of the lepton. Thus, the higher the lepton p_T, the smaller will be isolation cone, and the smaller will be the mini-isolation value. Originally, this variable has been designed to efficiently identify relatively high-p_T leptons overlapping with jets such as in semi-leptonic boosted top decays [47] and SUSY cascade decays [48]. In the fully hadronic SVJ search [44], the background from boosted top decays in semi-leptonic final states is reduced by applying a veto on mini-isolated leptons. However, this requirement removes almost all the SVJℓ signal and reduces, even if less drastically, also the SVJτ signal efficiency. This is because, especially for the SVJℓ signal, leptons are direct decay products of the dark bound states. Therefore, they are expected to be surrounded by SM hadrons coming from the hidden sector decays. Thus, they will be non-isolated, but they will have sufficiently high p_T to appear as mini-isolated. This effect is mitigated in the case of the SVJτ signature since final state leptons are expected to be softer because part of the energy of the original τ lepton coming from the dark bound states decays is carried away from the neutrinos from the τ lepton decay.

The second important limitation comes from the trigger strategy adopted. The triggers utilised are jet p_T and H_T based triggers. To have fully efficient triggers, a selection on the dijet transverse mass $m_T > 1.5\,\text{TeV}$ is required. This selection generally confines the search sensitivity to high Z' masses ($m_{Z'} \geq 1.5\,\text{TeV}$). Moreover, in the case of the SVJτ signature, the additional presence of

neutrinos enhancing the total effective invisible fraction in the event leads to a further broadening and shift of the signal mass peak towards lower m_T values, thus further spoiling the signal sensitivity and mass reach.

3.2. Custom Isolations and Leptons-Based Jet Observables

One first modification to the CMS analysis strategy to tackle the new signatures, and especially beneficial for the SVJℓ signature, is to remove the mini-isolation requirement, and use instead a custom targeted isolation, called inter-isolation [34]. This isolation measures the leptonic activity in a cone of fixed size around a given lepton: $I_{int}(\ell) = \sum_{\Delta R < R_{iso}} p_{T,\ell_j} / p_{T,\ell}$, where ℓ is the target lepton and ℓ_j are all the other leptons within a cone of radius R_{iso}. The variable I_{int} is expected to be larger for signal leptons due to their higher multiplicity in the signal jets compared to background jets. The inter-isolation variable provides good rejection against all the backgrounds. Furthermore, this variable captures the main feature of the SVJℓ leptons leading to a peak in the multiplicity for one pair of non inter-isolated leptons, as shown in Figure 3. Another important handle that can be exploited for the SVJℓ signature is the expected presence of at least one peak in the di-lepton invariant mass spectrum, as shown in Figure 3. This is a model-dependent feature since multiple resonances can appear according to the structure of the hidden sector. In principle, one can look for such resonances independently from the high mass Z' resonance, or look for both simultaneously.
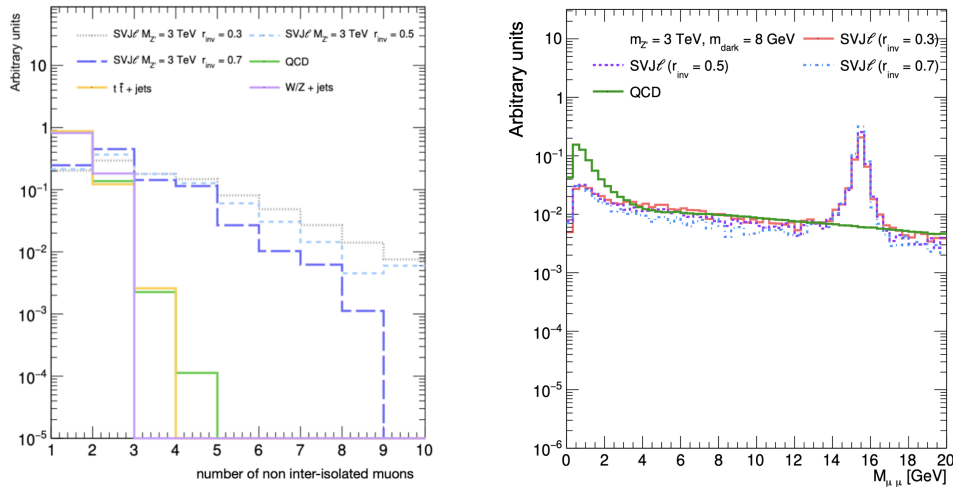

FIGURE 3: *Left panel*: multiplicity of non interisolated muons for different signal hypothesis and major backgrounds (from [34]). *Right panel*: invariant mass distribution from the two highest p_T non-interisolated muons in the event.

The SVJτ signature is in general more challenging from an experimental point of view due to a softer lepton spectrum, the presence of additional neutrinos from τ leptons decays and hadronic τ decays, which are difficult to distinguish inside a hadronic jet. Because the τ candidates for the signal are non-isolated, and with relatively low p_T, since they come from bound states with mass below the $b\bar{b}$ threshold, then their identification is hard with the current techniques. Nonetheless, it is possible to separate the signal jets from the background jets, exploiting the differences in the substructure. The enriched leptonic content of the signal jets especially suggests the design of new substructure variables leveraging such features. In [35], we propose new lepton-based jet-substructure variables that can be exploited as features by a jet tagger, in our case a Boosted Decision Tree (BDT). In our jet tagger, we exploit three main features of electrons and muons in signal jets: energy and momentum flow, spatial distribution, and isolation. For the first category of variables, energy fractions ($f(\ell)$) are used together with the average lepton p_T normalised by the jet transverse momentum ($p_{T,norm}(\ell)$). The second category of variables includes the radial distribution of electrons and muons concerning the jet axis normalised by the jet radius ($R_{norm}(\ell)$). Finally, the third class of variables includes the inter-isolation ($I_{int}(\ell)$), as well as a new isolation variable: $I_{\pi\gamma}(\ell)$. The isolation variable $I_{\pi\gamma}(\ell)$ is built by summing the momenta of all charged pions and photons reconstructed in the event within a cone of a given radius centred around the candidate lepton itself associated to a given jet, and then normalising to the lepton p_T. This variable aims to capture $\pi_v \rightarrow \tau(h)\tau(\ell)$ when the dark hadron π_v is boosted enough and the $\tau(h)$ products overlap with the lepton from $\tau(\ell)$. The list of input features used for the tagger are shown in Table 1. At the optimal working point, the tagger rejects $\sim$97% of simulated background jets, while correctly classifying $\sim$80–93% depending on the signal hypothesis. Figure 4 shows the BDT response for signal and background, showing a high separation between the two hypotheses. This high performance is achieved only by classifying jets according to their lepton content, and further improvements can be achieved by supplementing the set of variables proposed with the jet substructure variables used in [44].

3.3. Investigation on Possible New Trigger Strategies

As previously mentioned, for the SVJℓ signature, it is possible to look for the high mass resonance from the Z' searching for a bump in the dijet transverse mass, as well as look for possible resonances from dark vector bound states ρ_v decays in the low mass region

Rank	Variable	Definition
1	$I_{\text{int}}(\mu)$	$\sum_{\ell \neq \mu}^{\Delta R < R_{\text{iso}}} p_T(\ell)/p_T(\mu)$
2	$R_{\text{norm}}(\mu)$	$\sum_{\ell \in \text{jet}} \Delta R(\mu, \ell)/R$
3	$I_{\pi\gamma}(\mu)$	$\sum_{i \in \{\pi^\pm, \gamma\} \in \text{jet}}^{\Delta R < R_{\text{iso}}} p_T(i)/p_T(\mu)$
4	$R_{\text{norm}}(e)$	$\sum_{\ell \in \text{jet}} \Delta R(e, \ell)/R$
5	$I_{\text{int}}(e)$	$\sum_{\ell \neq e}^{\Delta R < R_{\text{iso}}} p_T(\ell)/p_T(e)$
6	$f(e)$	$\sum_{e \in \text{jet}} p_T(e)/\sum_{i \in \text{jet}} p_T(i)$
7	$I_{\pi\gamma}(e)$	$\sum_{i \in \{\pi^\pm, \gamma\} \in \text{jet}}^{\Delta R < R_{\text{iso}}} p_T(i)/p_T(e)$
8	$p_{T,\text{norm}}(\mu)$	$p_T(\mu)/p_T(\text{jet})$
9	$f(\mu)$	$\sum_{\mu \in \text{jet}} p_T(\mu)/\sum_{i \in \text{jet}} p_T(i)$

TABLE 1: Input variables to the jet tagger ordered by decreasing separation power (Table from [35]). In the third column are reported the definitions of the variables used with the following conventions: R is the jet radius, R_{iso} is the isolation cone radius.
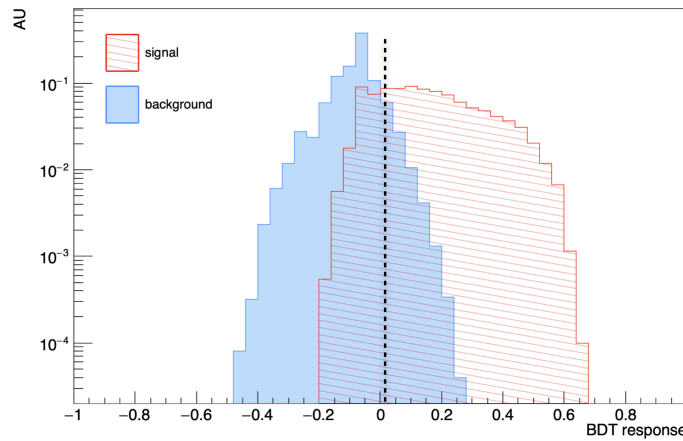

FIGURE 4: SVJτ tagger response (Figure from [35]). The vertical black dashed line represents the best cut value.

of the dilepton spectrum. For the high mass search in the dijet transverse mass, the same jet p_T and H_T based triggers used in [44] can be employed. For the low mass search, one would need to consider triggers imposing loose requirements on the transverse momentum of the lepton candidates and without standard relative isolation requirements. Relatively high masses for ρ_v might be accessible with current double-muon triggers, while the mass range below 20 GeV is not expected to be accessible with such standard triggers.

In the case of the SVJτ search, further challenges on the trigger side emerge. Indeed, the jet p_T and H_T based triggers used in [44] to be fully efficient require $m_T \geq 1.5$ TeV, which would remove largest part of the signal bulk for hypothesized Z' masses also up to 3 TeV, especially for large BR_τ values, thus spoiling the final sensitivity. The impact of such requirement is shown in Figure 5 for Z' masses of 1 TeV and 1.5 TeV. In [35], we have investigated alternative trigger strategies. The invisible component of the SVJτ signature would suggest the investigation of $\not{E}_T$ based triggers. However, the threshold for the lowest unprescaled $\not{E}_T$ trigger is $\mathcal{O}(200\,\text{GeV})$, thus for Z' masses below 2 TeV the signal efficiency is too low to achieve enough sensitivity. Tau triggers represent another physics-motivated set of triggers. Using single-τ triggers is not expected to be effective due to the tight isolation requirements of the τ candidates. Di-τ triggers have also been investigated since no isolation of the τ candidates is required above 25 GeV. However, due to the expected low p_T spectrum for the signal τ candidates, also di-τ triggers are expected to be inefficient.

Finally, a topological trigger using the pseudorapidity separation between jets was studied. This selection can be applied already at the first trigger level (L1), to reduce hadronic rates before the High Level Trigger (HLT). Comparing the acceptance of QCD background and signal events with and without the additional ΔR requirement, a larger decrease in the acceptance was observed for the background, as shown in Figure 5. These studies suggest that topological trigger strategies might aid in lowering the H_T trigger thresholds.

Hadronic trigger thresholds can also be lowered by using alternative data-taking workflows such as Data Parking [49] (delayed stream in ATLAS [50]), or Data Scouting [51] (Trigger-Level Analysis in ATLAS [52]). In Run 2, the latter technique only retained global information about the jets reconstructed at the HLT.
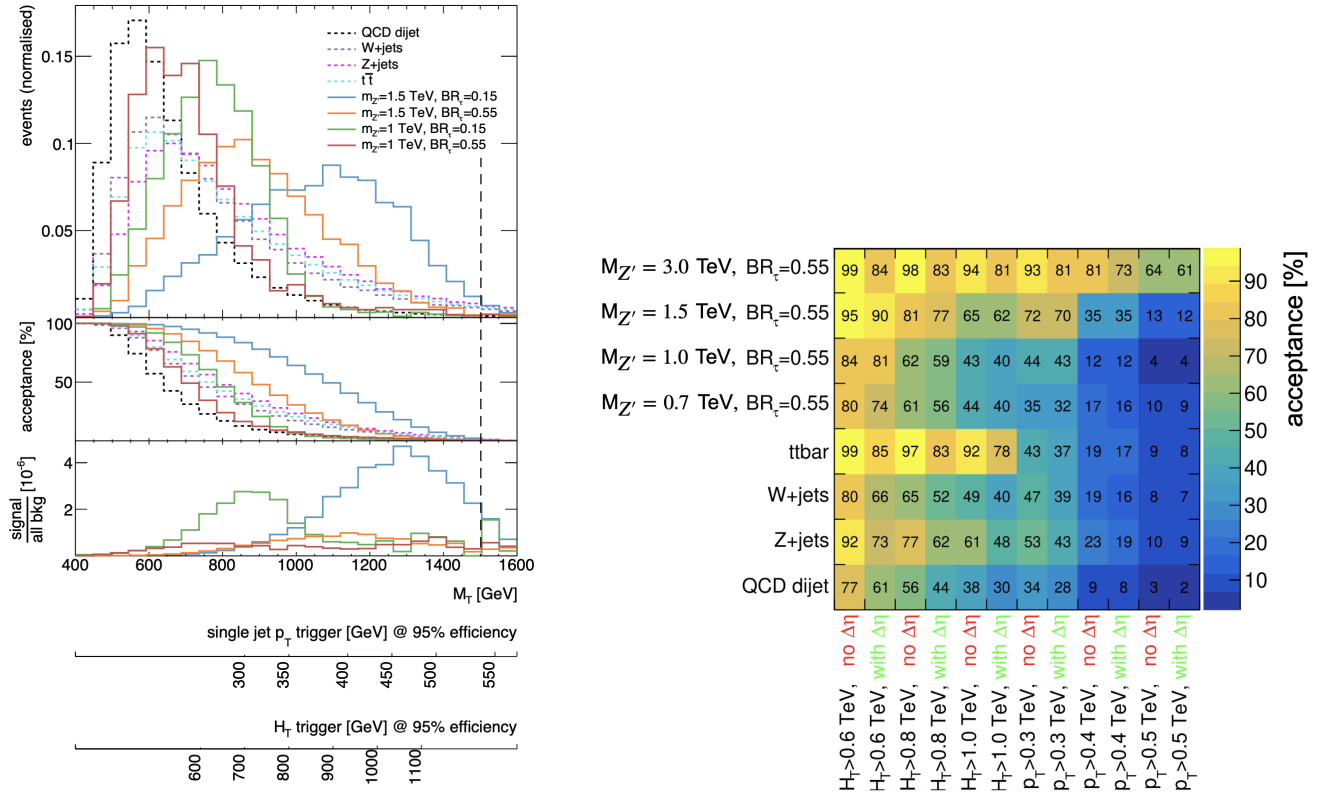
FIGURE 5: *Left panel*: transverse mass distributions for different signal hypothesis and backgrounds (from [35]). In the middle the acceptance and the bin-by-bin signal-to-background ratio are shown. The axes on the bottom of the plot show the M_T values at which various trigger selections have been determined to be 95% efficient. The vertical dashed lined represents the m_T selection applied in [44]. *Right panel*: efficiencies for signals and backgrounds for different values of the trigger threshold on H_T with and without topological requirements on the two leading jets pseudorapidity separation $\Delta \eta$ (from [35]).

4. RESULTS

For the SVJℓ signature, the left panel in Figure 6 shows the expected sensitivity reach applying the fully-hadronic inclusive analysis strategy in [44] and the targeted one we propose in [34]. Our study clearly shows that the discovery of the SVJℓ signal with full Run 2 data collected by the CMS experiment is not possible with the fully-hadronic analysis strategy. Thus, a new search is needed to tackle such a signature. The analysis strategy we propose, employing the inter-isolation variable, would allow us to achieve the necessary sensitivity to claim the evidence of a Z' boson up to 3.5 TeV and exclude it up to 4 TeV, with Run 2 LHC luminosity. Further improvements in the sensitivity reach can be achieved by exploiting the dimuon invariant mass and the dijet transverse mass in the fit, as shown in the right panel of Figure 6. With this strategy, the discovery of the signal is expected for Z' mass up to 5 TeV.

The results for the SVJτ signature are shown in Figure 7. From the left panel, it is shown that the CMS inclusive analysis strategy is not sufficient to probe the SVJτ signature. First, we show that employing a dedicated tagger based on the leptonic content of the signal jets allows to achieve the sensitivity for the discovery of the Z' in the SVJτ signature up to 4.5 TeV, and exclude it up to 5.5 TeV, with Run 2 LHC luminosity. Furthermore, employing an alternative trigger strategy for Run 3, lowering the m_T threshold down to 800 GeV would give access to possibly discover the Z' at lower masses down to 700 GeV. In the right panel, the expected limits on $\sigma \times \mathrm{Br}(Z' \rightarrow q_v \bar{q}_v)$ are translated into limits on g_u. For the proposed SVJτ, the suggested analysis would allow to probe the coupling of the hypothetical Z' to quarks like no other LHC search did previously.

5. CONCLUSIONS

We have proposed new simplified models and signatures for confining dark sectors resulting in leptons-enriched semi-visible jets. Allowing the dark bound states to decay also leptonically opens the doors to new experimental handles that can be exploited in order to search for these anomalous jets in the extremely busy hadronic environment of the LHC. Beyond the very attractive new dimuon resonances at low mass due to dark vector mesons ρ_v decays offered by the SVJℓ signature, we proposed new custom lepton isolation variables and lepton-based jet observables that are powerful for discriminating the signal jets from the overwhelm-
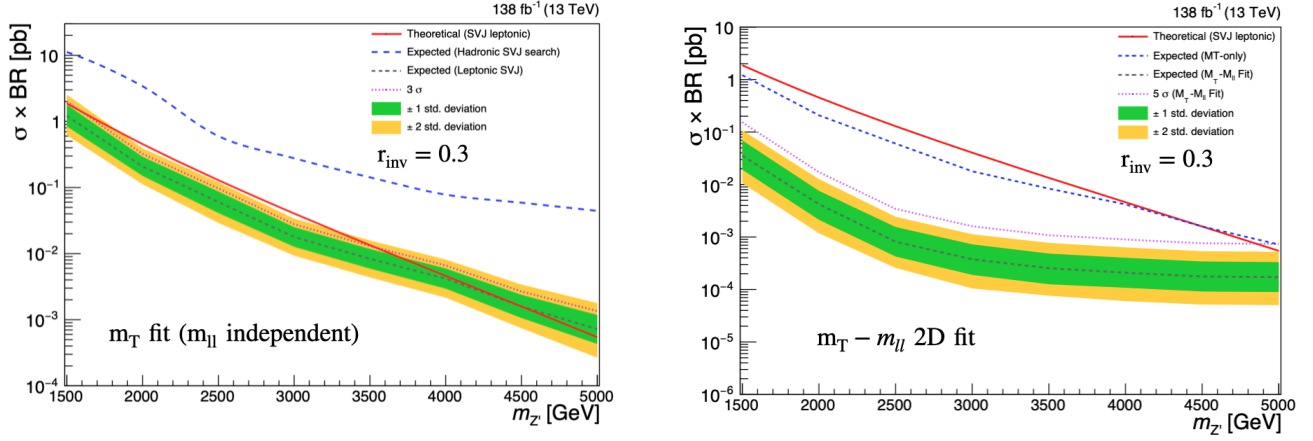
FIGURE 6: Expected limits for SVJℓ signature on $\sigma \times \mathrm{BR}(Z' \to q_v \bar{q}_v)$ for the signal benchmark with Delphes samples. *Left panel*: expected limits fitting m_T distribution (Figure from [34]). The blue dashed line represents the expected exclusion at 95% CL applying the fully-hadronic analysis strategy from CMS [44] on the SVJℓ signature. The grey dashed line represents the exclusion reach with the targeted analysis proposed in [34]. *Right panel*: the expected limit fitting m_T vs m_{ll} 2D distribution is represented by the grey line, and it is compared to the m_T-only fit of the SVJℓ targeted analysis (blue dashed line).
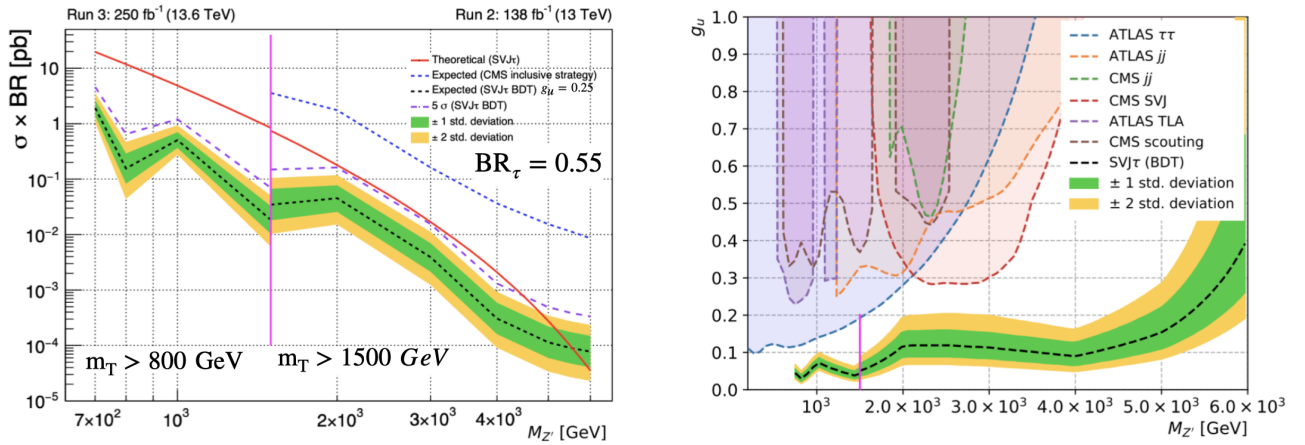

FIGURE 7: Expected limits for SVJτ signature for the signal benchmark with Delphes samples. *Left panel*: expected limits on $\sigma \times \mathrm{Br}(Z' \to q_v \bar{q}_v)$ fitting m_T distribution (Figure from [35]). The blue dashed line represents the expected exclusion at 95% CL applying the fully-hadronic analysis strategy from CMS [44] on the SVJτ signature. The grey dashed line represents the exclusion reach with the targeted analysis proposed in [35]. The vertical magenta line separates the two posible trigger strategies: $m_T > 1.5\,\mathrm{TeV}$ for Run 2 emplying same triggers as in [44], and $m_T > 0.8\,\mathrm{TeV}$ with alternative trigger strategies for Run 3. *Right panel*: expected limits on the coupling of Z' to quarks g_u (Figure from [35]).

ing hadronic background. Looking for these new signatures is also an experimental challenge, especially from the perspective of efficient triggers that can be employed. We reviewed some limitations of the current triggers, and proposed possible alternative strategies that can be tested by the experimental collaborations. Leptons-enriched signatures and models are mildly constrained by the current LHC searches, thus they represent an important opportunity for Hidden Valleys discovery at particles colliders.

ACKNOWLEDGMENTS

References

[1] Gianfranco Bertone, Dan Hooper, and Joseph Silk. Particle dark matter: Evidence, candidates and constraints. *Phys. Rept.*, 405:279–390, 2005.

[2] N. Aghanim, Y. Akrami, M. Ashdown, J. Aumont, C. Baccigalupi, M. Ballardini, A. J. Banday, R. B. Barreiro, N. Bartolo, S. Basak, R. Battye, K. Benabed, and et al. Planck 2018 results. *Astronomy & Astrophysics*, 641:A6, Sep 2020.

[3] Benjamin W. Lee and Steven Weinberg. Cosmological lower bound on heavy-neutrino masses. *Phys. Rev. Lett.*, 39:165–168, Jul 1977.

[4] Gerard Jungman, Marc Kamionkowski, and Kim Griest. Supersymmetric dark matter. *Phys. Rept.*, 267:195–373, 1996.

[5] Armen Tumasyan et al. Search for new particles in events with energetic jets and large missing transverse momentum in proton-proton collisions at $\sqrt{s} = 13$ TeV. *JHEP*, 11:153, 2021.

[6] Georges Aad et al. Search for new phenomena in events with an energetic jet and missing transverse momentum in pp collisions at $\sqrt{s} = 13$ TeV with the ATLAS detector. *Phys. Rev. D*, 103(11):112006, 2021.

[7] Albert M. Sirunyan et al. Search for new physics in final states with a single photon and missing transverse momentum in proton-proton collisions at $\sqrt{s} = 13$ TeV. *JHEP*, 02:074, 2019.

[8] Armen Tumasyan et al. Search for new physics in the lepton plus missing transverse momentum final state in proton-proton collisions at $\sqrt{s} = 13$ TeV. 2, 2022.

[9] Albert M. Sirunyan et al. Search for dark matter produced in association with a leptonically decaying Z boson in proton-proton collisions at $\sqrt{s} = 13$ TeV. *Eur. Phys. J. C*, 81(1):13, 2021. [Erratum: Eur.Phys.J.C 81, 333 (2021)].

[10] Georges Aad et al. Search for dark matter in events with a Z boson and missing transverse momentum in pp collisions at $\sqrt{s} = 8$ TeV with the ATLAS detector. *Phys. Rev. D*, 90(1):012004, 2014.

[11] Georges Aad et al. Search for dark matter produced in association with a single top quark in $\sqrt{s} = 13$ TeV pp collisions with the ATLAS detector. *Eur. Phys. J. C*, 81(10):860, 2021.

[12] Albert M. Sirunyan et al. Search for dark matter produced in association with a single top quark or a top quark pair in proton-proton collisions at $\sqrt{s} = 13$ TeV. *JHEP*, 03:141, 2019.

[13] Albert M. Sirunyan et al. Search for dark matter particles produced in association with a Higgs boson in proton-proton collisions at $\sqrt{s} = 13$ TeV. *JHEP*, 03:025, 2020.

[14] Georges Aad et al. Search for dark matter produced in association with a Standard Model Higgs boson decaying into b-quarks using the full Run 2 dataset from the ATLAS detector. *JHEP*, 11:209, 2021.

[15] Matthew J. Strassler and Kathryn M. Zurek. Echoes of a hidden valley at hadron colliders. *Phys. Lett. B*, 651:374–379, 2007.

[16] Hugues Beauchesne, Enrico Bertuzzo, and Giovanni Grilli Di Cortona. Dark matter in Hidden Valley models with stable and unstable light dark mesons. *JHEP*, 04:118, 2019.

[17] Elias Bernreuther, Felix Kahlhoefer, Michael Krämer, and Patrick Tunney. Strongly interacting dark sectors in the early Universe and at the LHC through a simplified portal. *JHEP*, 01:162, 2020.

[18] Graham D. Kribs and Ethan T. Neil. Review of strongly-coupled composite dark matter models and lattice simulations. *Int. J. Mod. Phys. A*, 31(22):1643004, 2016.

[19] Nathaniel Craig, Andrey Katz, Matt Strassler, and Raman Sundrum. Naturalness in the Dark at the LHC. *JHEP*, 07:105, 2015.

[20] Simon Knapen, Jessie Shelton, and Dong Xu. Perturbative benchmark models for a dark shower search program. *Phys. Rev. D*, 103(11):115013, 2021.

[21] Guillaume Albouy et al. Theory, phenomenology, and experimental avenues for dark showers: a Snowmass 2021 report. *Eur. Phys. J. C*, 82(12):1132, 2022.

[22] Cari Cesarotti, Matthew Reece, and Matthew J. Strassler. The efficacy of event isotropy as an event shape observable. *JHEP*, 07:215, 2021.

[23] Cari Cesarotti, Matthew Reece, and Matthew J. Strassler. Spheres To Jets: Tuning Event Shapes with 5 d Simplified Models. *JHEP*, 05:096, 2021.

[24] Simon Knapen, Simone Pagan Griso, Michele Papucci, and Dean J. Robinson. Triggering Soft Bombs at the LHC. *JHEP*, 08:076, 2017.

[25] Matthew J. Strassler. Why Unparticle Models with Mass Gaps are Examples of Hidden Valleys. 1, 2008.

[26] Pedro Schwaller, Daniel Stolarski, and Andreas Weiler. Emerging Jets. *JHEP*, 05:059, 2015.

[27] Morad Aaboud et al. Search for long-lived neutral particles in pp collisions at $\sqrt{s} = 13$ TeV that decay into displaced hadronic jets in the ATLAS calorimeter. *Eur. Phys. J. C*, 79(6):481, 2019.

[28] Myeonghun Park and Mengchao Zhang. Tagging a jet from a dark sector with Jet-substructures at colliders. *Phys. Rev. D*, 100(11):115009, 2019.

[29] Timothy Cohen, Joel Doss, and Marat Freytsis. Jet Substructure from Dark Sector Showers. *JHEP*, 09:118, 2020.

[30] Timothy Cohen, Mariangela Lisanti, and Hou Keong Lou. Semivisible Jets: Dark Matter Undercover at the LHC. *Phys. Rev. Lett.*, 115(17):171804, 2015.

[31] Timothy Cohen, Mariangela Lisanti, Hou Keong Lou, and Siddharth Mishra-Sharma. LHC Searches for Dark Sector Showers. *JHEP*, 11:196, 2017.

[32] Search for resonant production of strongly-coupled dark matter in proton-proton collisions at 13 TeV. 2021.

[33] Search for non-resonant production of semi-visible jets using Run 2 data in ATLAS. 2022.

[34] Cesare Cazzaniga and Annapaola de Cosa. Leptons lurking in semi-visible jets at the LHC. *Eur. Phys. J. C*, 82(9):793, 2022.

[35] Hugues Beauchesne, Cesare Cazzaniga, Annapaola de Cosa, Caterina Doglioni, Tobias Fitschen, Giovanni Grilli di Cortona, and Ziyuan Zhou. Uncovering tau leptons-enriched semi-visible jets at the LHC. *Eur. Phys. J. C*, 83(7):599, 2023.

[36] David Curtin, Rouven Essig, Stefania Gori, and Jessie Shelton. Illuminating Dark Photons with High-Energy Colliders. *JHEP*, 02:157, 2015.

[37] Georges Aad et al. Search for high-mass dilepton resonances using 139 fb^{-1} of pp collision data collected at $\sqrt{s} = 13$ TeV with the ATLAS detector. *Phys. Lett. B*, 796:68–87, 2019.

[38] Albert M. Sirunyan et al. Search for a Narrow Resonance Lighter than 200 GeV Decaying to a Pair of Muons in Proton-Proton Collisions at $\sqrt{s} =$ TeV. *Phys. Rev. Lett.*, 124(13):131802, 2020.

[39] Search for prompt production of a GeV scale resonance decaying to a pair of muons in proton-proton collisions at $sqrts = 13$ TeV. 2023.

[40] Roel Aaij et al. Search for $A' \rightarrow \mu^+\mu^-$ Decays. *Phys. Rev. Lett.*, 124(4):041801, 2020.

[41] Georges Aad et al. Search for new resonances in mass distributions of jet pairs using 139 fb^{-1} of pp collisions at $\sqrt{s} = 13$ TeV with the ATLAS detector. *JHEP*, 03:145, 2020.

[42] Albert M. Sirunyan et al. Search for high mass dijet resonances with a new background prediction method in proton-proton collisions at $\sqrt{s} = 13$ TeV. *JHEP*, 05:033, 2020.

[43] Morad Aaboud et al. Search for additional heavy neutral Higgs and gauge bosons in the ditau final state produced in $36\,\text{fb}^{-1}$ of pp collisions at $\sqrt{s} = 13$ TeV with the ATLAS detector. *JHEP*, 01:055, 2018.

[44] Armen Tumasyan et al. Search for resonant production of strongly coupled dark matter in proton-proton collisions at 13 TeV. *JHEP*, 06:156, 2022.

[45] M. Aaboud et al. Search for low-mass dijet resonances using trigger-level jets with the ATLAS detector in pp collisions at $\sqrt{s} = 13$ TeV. *Phys. Rev. Lett.*, 121(8):081801, 2018.

[46] Albert M. Sirunyan et al. Search for narrow and broad dijet resonances in proton-proton collisions at $\sqrt{s} = 13$ TeV and constraints on dark matter mediators and other new particles. *JHEP*, 08:130, 2018.

[47] Keith Rehermann and Brock Tweedie. Efficient Identification of Boosted Semileptonic Top Quarks at the LHC. *JHEP*, 03:059, 2011.

[48] Albert M. Sirunyan et al. Search for supersymmetry in pp collisions at $\sqrt{s} = 13$ TeV with $137\,\text{fb}^{-1}$ in final states with a single lepton using the sum of masses of large-radius jets. *Phys. Rev. D*, 101(5):052010, 2020.

[49] Data Parking and Data Scouting at the CMS Experiment, 2012.

[50] Georges Aad et al. Search for new phenomena in the dijet mass distribution using p-p collision data at $\sqrt{s} = 8$ TeV with the ATLAS detector. *Phys. Rev. D*, 91(5):052007, 2015.

[51] The CMS Collaboration. Search for dijet resonances in proton-proton collisions at $s = 13$ TeV and constraints on dark matter and other models. *Physics Letters B*, 769:520–542, 2017.

[52] ATLAS Collaboration. Search for low-mass dijet resonances using trigger-level jets with the atlas detector in pp collisions at $\sqrt{s} = 13$ TeV. *Phys. Rev. Lett.*, 121:081801, Aug 2018.